Journal Pre-proof

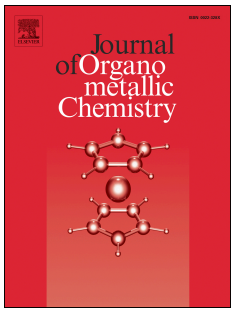

Ruthenium, rhodium and iridium complexes containing pyrimidine based thienyl pyrazoles: Synthesis and antibacterial studies

Agreeda Lapasam, Ibaniewkor L. Mawnai, Venkanna Banothu, Werner Kaminsky, Mohan Rao Kollipara

PII: S0022-328X(20)30056-5

DOI: https://doi.org/10.1016/j.jorganchem.2020.121155

Reference: JOM 121155

To appear in: *Journal of Organometallic Chemistry*

Received Date: 23 November 2019

Revised Date: 3 February 2020

Accepted Date: 3 February 2020

Please cite this article as: A. Lapasam, I.L. Mawnai, V. Banothu, W. Kaminsky, M.R. Kollipara, Ruthenium, rhodium and iridium complexes containing pyrimidine based thienyl pyrazoles: Synthesis and antibacterial studies, *Journal of Organometallic Chemistry* (2020), doi: https://doi.org/10.1016/j.jorganchem.2020.121155.

Ruthenium, rhodium and iridium complexes containing pyrimidine based thienyl pyrazoles: Synthesis and antibacterial studies

Agreeda Lapasam[a], Ibaniewkor L. Mawnai[a], Venkanna Banothu[b], Werner Kaminsky[c], Mohan Rao Kollipara[a]*

[a]*Centre for Advanced Studies in Chemistry, North-Eastern Hill University, Shillong-793 022, India.*

[b]*Centre for Biotechnology (CBT), Institute of Science & Technology (IST), Jawaharlal Nehru Technological University Hyderabad (JNTUH), Kukatpally-500 085, Hyderabad, Telangana State, India.*

[c]Department of Chemistry, University of Washington, Seattle, WA 98195, USA

E-mail: mohanrao59@gmail.com

Graphical abstract

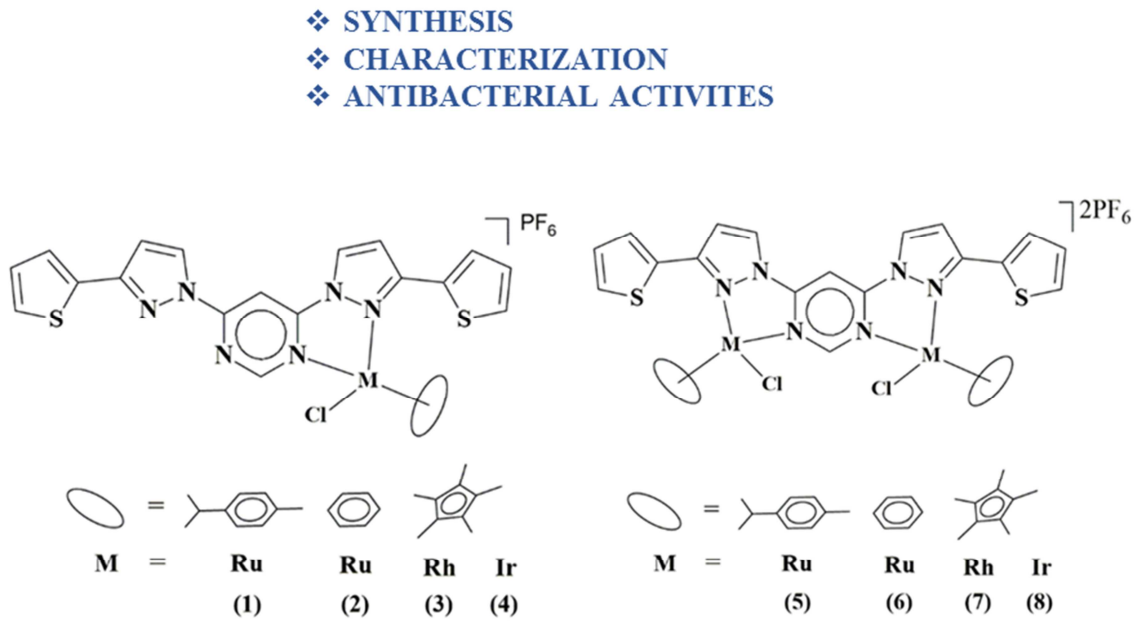

Abstract

The reaction of pyrimidine based electron-rich heterocyclic thiophene pyrazoles and halide bridged arene d^6 metal precursors yielded a series of mononuclear and dinuclear half sandwich d^6 metal complexes. Mononuclear and dinuclear complexes formed by the ratio-based reaction between ligand and metal precursor. All these cationic complexes have been characterized by IR, UV–Vis, ^{1}H NMR, ^{13}C NMR spectroscopic techniques. Complex **5** has been established by single-crystal analysis. X-ray diffraction studies revealed the formation of mononuclear and dinuclear complexes and suggest that the vicinity around the metal atom is distorted octahedral. An *in vitro* study to screen the antibacterial potential of these complexes against pathogenic bacteria, *S. aureus, K. pneumoniae,* and *E. coli* was addressed. All the complexes display a better zone of inhibitions for both Gram-positive (*S. aureus*) and Gram-negative strains (*K. pneumoniae*, and *E. coli*). The minimum inhibitory concentrations (MICs) for the most active complex ranged from 0.125 to 0.25 mg/ml for *S. aureus* and *Klebsiella Pneumoniae* and 0.25 to 0.5 mg/ml for *E. coli*.

Keywords: Ruthenium, Rhodium, Iridium, Antibacterial studies.

1. Introduction

Bacterial resistance to antimicrobial drugs is a significant threat to humans [1]. Infectious diseases caused by drug-resistant bacteria are currently the second main cause of death worldwide and the third leading cause of death in developed countries. Due to the increasing resistance of bacteria to the current clinical drugs, there has been increasing interest in the development of novel classes of antimicrobials agents that may not be as susceptible to the bacterial mechanisms of resistance developed against the current range of drugs [2-6]. Based on the comparative success of platinum group metal complexes as anticancer agents, there is a rising attention in the use of metal complexes as antimicrobial agents [7-9]. Ruthenium complexes exhibit a wide range of properties and a large variety of ruthenium complexes have found applications in biological and pharmaceutical studies such as antibacterial, antifungal, antimalarial, anti-proliferative, anti-inflammatory, antiviral and antipyretic activities [10-15]. Cp*Rh and Cp*Ir complexes have also been considered as alternatives to ruthenium-based drugs because of their biological applications and their water solubility. A well-defined series of metal complexes with antibacterial activity is that of rhodium(III) coordination compounds of formula *trans*-$[RhX_2(Py)_4]Y$ [16-17]. Pharmaceuticals focusing on metal complexes of iridium are still at the early stages [18]. Medically, organometallic complexes of iridium(III) proved to have potentials for anticancer and antimicrobial activities [19]. Cyclometallated iridium(III) complexes bearing dithiocarbamate derivatives have been reported to possess antibacterial activity [20]. The delocalization of the π-electrons over the chelate ring was proposed to increase the lipophilicity of the complexes and facilitate their penetration into bacterial cell membranes, thereby resulting in inhibition of bacterial growth.

Since the development of coordination chemistry, various new chelating N heterocyclic ligands have been synthesized. Because of wide range of applications, new ruthenium complexes with different types of ligands are of particular interest. A family of nitrogen-containing pyrazole based ligands has been widely studied and offered a diversity of applications [21]. There have been reports on pyrimidyl pyrazole derivatives being used as antitumor agents and show the antiproliferative effect on human lung cancer cell line as well as inhibited the polymerization of tubulin. The most probable way in which pyrazole based compounds exhibit bioactivity is by the formation of a hydrogen bond with biomolecules [22-24]. Organometallic complexes containing such ligands are considered as potential DNA intercalators with the capability to inhibit the synthesis of nucleic acid. When the strong σ-donor ability of pyrazole group and π-accepting property of pyrimidine ring are joined together, it may give rise to properties different from those of the isolated moieties.

In recent years, we have reported many organometallic complexes including half-sandwich platinum group metal complexes containing pyrazole ligands [25]. In continuation to our previous work, herein we report the synthesis of mono and binuclear arene ruthenium, rhodium, and iridium complexes containing pyrazole derivatives. The ligand used in this study is shown in (Chart 1).

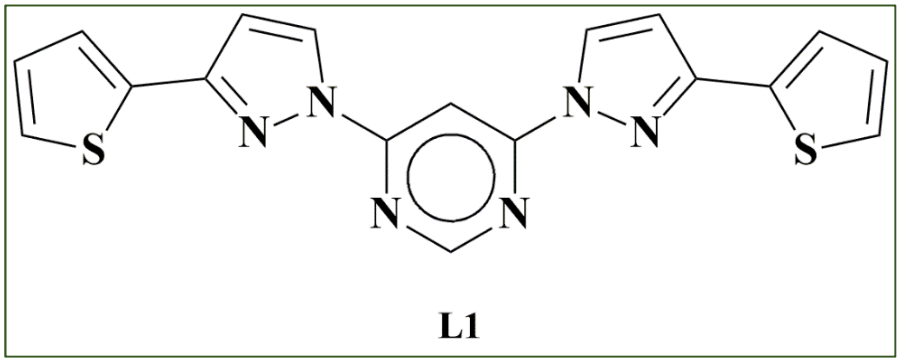

Chart 1: Ligand used in the present study.

2. Experimental Section

2.1. Physical methods and materials

All reagents used in this work were purchased commercially and used without further purification; Tetra-n-butylammonium bromide, 2 acetyl thiophene, 4, 6- dichloro pyrimidine were purchased from Sigma Aldrich. N, N- dimethylformamide dimethyl acetal was obtained from Spectrochem Pvt. limited, potassium carbonate was obtained from SD Fine-Chem limited, and hydrazine hydrate was purchased from Qualigens Fine Chemicals. Pentamethylcyclopentadiene and α-Terpinene were obtained from Sigma Aldrich. The solvents were purified and dried according to standard procedures [26]. The starting precursor metal complexes [(*p*-cymene)$RuCl_2]_2$, [(benzene)$RuCl_2]_2$, and [Cp*$MCl_2]_2$ (M = Rh/Ir) were prepared according to the literature methods [27-29]. The syntheses of all the metal complexes were performed at room temperature. Infrared (IR) spectra were recorded on a Bruker ALPHA II FTIR spectrometer as KBr pellets in the range 4000 to 400 cm^{-1}. ^1H NMR spectra were recorded on a Bruker Avance II 400 MHz spectrometer using $CDCl_3$ and DMSO-d_6 as solvents, with TMS as internal references. UV–Vis absorption spectra were obtained on a Perkin-Elmer Lambda 25 UV/Vis spectrophotometer in acetonitrile solution. Elemental analyses of the complexes were carried out on a Perkin-Elmer 2400 CHN analyzer.

2. 2 Single-crystal X-ray structures analyses

Suitable single crystals of complex **5** were obtained by slow diffusion of hexane into acetone solution. Single crystal X-ray diffraction data for the complexes were collected on an Oxford Diffraction Xcalibur Eos Gemini diffractometer at 293 K using graphite monochromated Mo-Kα radiation (λ = 0.71073 Å). The strategy for the data collection was evaluated using the CrysAlisPro CCD software. Crystal data were collected by standard ‘‘phi–omega scan’’

techniques and were scaled and reduced using CrysAlisPro RED software. The structures were solved with the SHELXT-2016 [30] solution program using the direct method and refined full-matrix least-squares with SHELXL-2016 refining on F^2 [31]. The positions of all the atoms were obtained by direct methods. Metal atoms in the complex were located from the E-maps and non-hydrogen atoms were refined anisotropically. Crystallographic and structure refinement parameters for the complexes are summarized in Table 1, and selected bond lengths and bond angles are presented in Table 2. The molecular structure of complex **5** is presented as thermal ellipsoid plot in Figure 1 [32].

2.3 Antimicrobial activity

All the Gram-negative and Gram-positive bacterial strains used for the present study were obtained from the Department of Microbiology, Osmania General Hospital, Hyderabad. All strains were tested for purity by standard microbiological methods. The bacterial stock cultures were maintained on Mueller-Hinton agar slants and stored at 4˚C. An agar-well diffusion method was employed for the evaluation of antibacterial activities of test compounds [33]. DMSO was used as a negative control. The bacterial strains were reactivated from stock cultures by transferring into Mueller-Hinton broth and incubating at 37 ˚C for 18 h. A final inoculum containing 10^6 colonies forming units (1 x 10^6 CFU/ml) was added aseptically to MHA medium and poured into sterile Petri dishes. Different test compounds at a concentration of 100 µg per well were added to wells (8 mm in diameter) punched on the agar surface. Plates were incubated overnight at 37 ºC and the diameter of inhibition zone (DIZ) around each well was measured in mm. Experiments were performed in triplicates (Error bars with percentage and standard deviation)

2.4 MIC and MBC

The minimum inhibitory concentration (MIC) and minimum bactericidal concentration (MBC) was determined by the micro-broth dilution method done in 96 well plates according to the standard protocol [34]. A 2-fold serial dilution of the compounds, with the appropriate antibiotic, was prepared. Initially, 100 µl of MH broth was added to each well plate. Then 100 µl of compound or antibiotic was taken from the stock solution and dissolved in the first well plate. Serial dilution was done to obtain different concentrations. The stock concentrations of 2.0 mg/ml. 24 hr culture turbidity was adjusted to match 0.5 McFarland standards which correspond to 1×10^{8} CFU/ml. The standardized suspension (100 µl) of bacteria was added to all the wells except the antibiotic control well and the 96 well plates were incubated at 37 °C for 24 h. After 24 h of incubation 40 µl of MTT (3-(4,5-dimethlthiazol-2-yl)-2,5-diphenyltetrazolium bromide) reagent (0.1 mg/ml in 1x PBS) was added to all the wells. MIC was taken as the lowest concentration which did not show any growth which was visually noted from the blue color developed by MTT. Subcultures were made from clear wells and the lowest concentration that yielded no growth after subculturing was taken as the MBC.

2.5. Synthesis of ligand (L1)

The ligand (L1) was synthesized following the reported method [25(a)]. 4,6-dichloro pyrimidine (2 mmol), thienyl pyrazole (4 mmol), potassium carbonate (4.5 mmol) and tetrabutylammonium bromide (4 mmol) were dissolved in 50 ml of acetone (Scheme-1). The reaction mixture was heated to reflux for 48h after the reaction completed the solvent was reduced, poured into distilled water and then extracted with DCM. The combined organic layer was dried over sodium sulfate (Na_2SO_4). The solvent was removed under vacuum and the resulting residue was purified by column chromatography using ethyl acetate and hexane (2:8 ratio) as eluent.

^{1}H NMR (400 MHz, $CDCl_3$, ppm): 10.85 (s, 1H), 10.20(s, 1H), 8.19 (d, 2H, *J* = 4 Hz), 8.00 (s, 2H), 7.31 (d, 2H, *J* = 4 Hz), 7.11 (d, 2H, *J* = 4 Hz), 6.41(s, 2H).

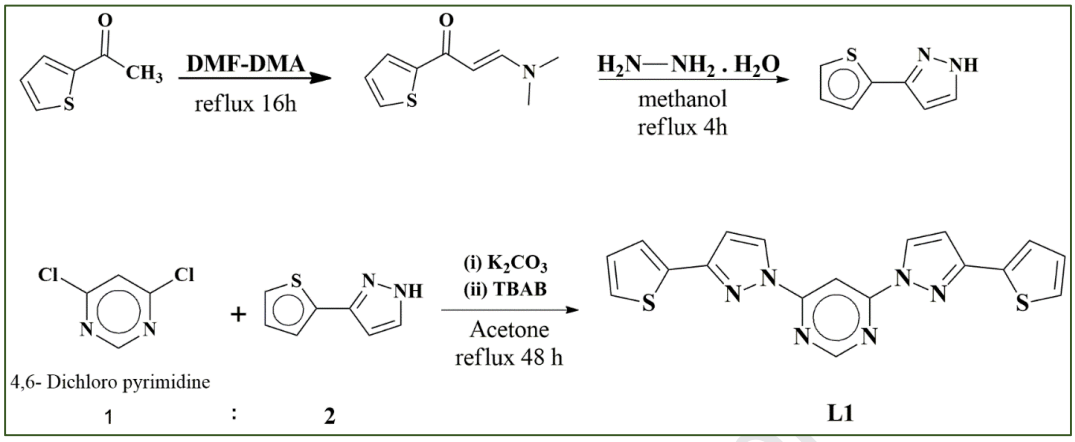

Scheme 1: Synthesis of ligand **L1**

*2.6. General procedure for the synthesis of mononuclear complexes **1-4***

A mixture of starting metal precursor (0.1 mmol) and ligand pyrimidine based thienyl pyrazoles (**L1**) (0.2 mmol) and 2.5 equivalents of NH_4PF_6 were dissolved in dry methanol (15 ml) and stirred at room temperature for 8 hours (Scheme-2). The solvent was evaporated to dryness. The residue was then dissolved in dichloromethane and filtered through a bed of celite to remove excess NH_4Cl. The filtrate was concentrated to 1 ml and on the addition of excess hexane yellow solid precipitates out. The precipitate was further washed with diethyl ether and air-dried.

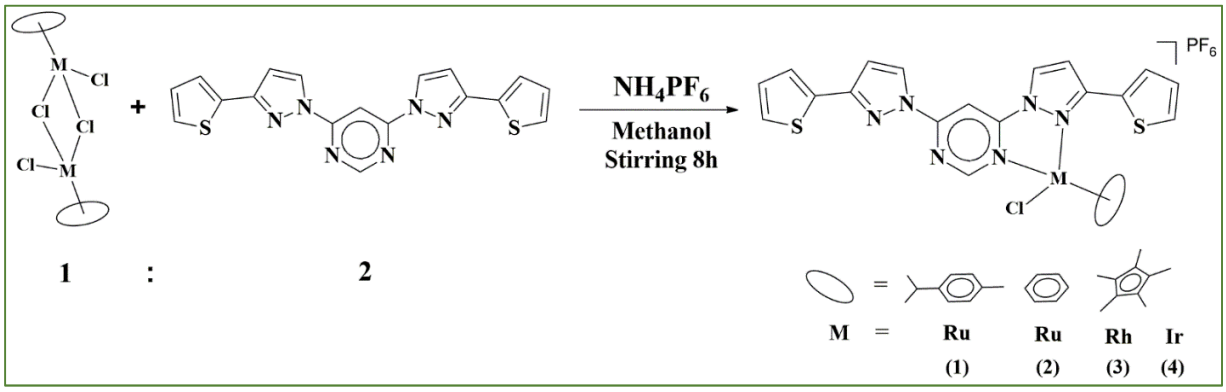

Scheme 2: Synthesis of complexes **1-4**

2.6.1. [(p-cymene)RuL1Cl]PF_6 ***[1]***

Yield: 80%; IR (KBr, cm^{-1}): 2967 $\nu_{(C-H)}$, 1587 $\nu_{(C=N)}$, 1116 $\nu_{(C-N)}$, 957 $\nu_{(N-N)}$, 844$\nu_{(P-F)}$, 789 $\nu_{(C-S)}$; ^1H NMR (400 MHz, $CDCl_3$, ppm) : 9.73 (s, 1H), 9.23 (s, 1H), 8.70 (t, 4H, *J* = 4 Hz), 8.21 (s, 1H), 7.86 (s, 1H), 7.67 (s, 1H), 7.57 (d, 2H, *J* = 4Hz), 6.92 (s,1H), 6.06 (d, 2H, *J* = 4 Hz), 6.03 (d, 2H, *J* = 4 Hz), 2.21 (sept, 1H), 1.79 (s, 3H), 1.12 (d, 6H, *J* = 4Hz); ^{13}C NMR (100 MHz,$CDCl_3$, ppm): 161.92,157.45, 153.97, 146.18, 143.72, 141.47, 129.25, 128.25, 127.90, 126.74, 104.84, 102.15, 101.08, 100.59, 86.92, 85.83, 85.52, 84.50, 30.87, 22.00, 17.94; UV-Vis {Acetonitrile, λ_{max} nm (ε/10-4 M^{-1} cm^{-1})}: 275.98 (6.48). Anal. Calc for $C_{28}H_{26}ClN_6RuS_2PF_6$ (792.16); C, 42.45; H, 3.31; N, 10.61. Found: C, 42.49; H, 3.29; N, 10.65 %.

2.6.2. [(benzene)RuL1Cl]PF_6 ***[2]***

Yield: 76%; IR (KBr, cm^{-1}): 2972 $\nu_{(C-H)}$, 1588 $\nu_{(C=N)}$, 1122 $\nu_{(C-N)}$, 959 $\nu_{(N-N)}$, 835$\nu_{(P-F)}$, 778 $\nu_{(C-S)}$; ^1H NMR (400 MHz, $CDCl_3$, ppm) : 11.39 (s, 1H), 8.68 (s, 1H), 7.92 (s, 1H), 7.85 (d, 1H, *J* = 4Hz), 7.51 (d, 1H, *J* = 4Hz), 7.23 (d, 1H, *J* = 4Hz), 7.01 (t, 1H, *J* = 4Hz), 6.69 (t, 1H, *J* = 4Hz), 6.57 (s, 3H, J = 8Hz), 6.21 (s, 1H), 5.98 (s, 6H); ^{13}C NMR (100 MHz,$CDCl_3$, ppm): 161.40, 158.96, 150.22, 144.87, 131.92, 131.66, 129.28, 128.42, 127.16, 125.22, 121.58, 108.88, 106.45, 86.56; UV-Vis {Acetonitrile, λ_{max} nm (ε/10-4 M^{-1} cm^{-1})}: 274.99 (7.86). Anal. Calc for $C_{24}H_{18}ClN_6RuS_2PF_6$ (736.06); C, 39.16; H, 2.46; N, 11.42. Found: C, 39.20; H, 2.48; N, 11.41 %.

*2.6.3. [Cp*RhL1Cl]PF_6* ***[3]***

Yield: 78%; IR (KBr, cm^{-1}): 2995 $\nu_{(C-H)}$, 1606 $\nu_{(C=N)}$, 1081 $\nu_{(C-N)}$, 955 $\nu_{(N-N)}$, 843$\nu_{(P-F)}$, 720 $\nu_{(C-S)}$; ^1H NMR (400 MHz, $CDCl_3$, ppm) :11.24 (s, 1H), 7.97 (s, 2H), 7.73 (s, 1H), 7.56 (d, 1H, *J* = 4Hz), 7.15 (d, 1H, *J* = 4Hz), 7.08 (d, 1H, *J* = 4Hz), 6.97 (t, 1H, *J* = 4Hz), 6.86 (t, 1H, *J* = 4Hz), 6.65 (d,

2H, J = 8Hz), 6.17 (s, 1H), 1.65 (s,15H); UV-Vis {Acetonitrile, λ_{max} nm (ε/10-4 M^{-1} cm^{-1})}: 234.99 (2.78), 274.98 (4.98). Anal. Calc for $C_{28}H_{27}ClN_6RhS_2PF_6$ (795.01); C, 42.30; H, 3.42; N, 10.57. Found: C, 42.28; H, 3.45; N, 10.60 %.

*2.6.4. [Cp*IrL1Cl]PF_6* ***[4]***

Yield: 69%; IR (KBr, cm^{-1}): 2967 $\nu_{(C-H)}$, 1577 $\nu_{(C=N)}$, 1121 $\nu_{(C-N)}$, 957 $\nu_{(N-N)}$, 844$\nu_{(P-F)}$, 786 $\nu_{(C-S)}$; ^{1}H NMR (400 MHz, $CDCl_3$, ppm): 11.24 (s, 1H), 7.97 (s, 1H), 7.74 (s, 1H), 7.56 (d, 1H, *J* = 4Hz), 7.15 (d, 1H, *J* = 4Hz), 7.08 (d, 1H, *J* = 4Hz), 6.97 (t, 1H, *J* = 4Hz), 6.86 (t, 1H, *J* = 4Hz), 6.64 (s, 3H, J = 8Hz), 6.17 (d, 1H), 1.79 (s,15H); ^{13}C NMR (100 MHz,$CDCl_3$, ppm): 166.26, 160.59, 154.00,145.09, 142.29, 138.93, 132.29, 129.09, 128.23, 123.89, 106.72, 104.84, 97.27, 13.42; UV-Vis {Acetonitrile, λ_{max} nm (ε/10-4 M^{-1} cm^{-1})}: 229.44 (4.05), 269.96 (2.35); Anal. Calc for $C_{28}H_{27}ClN_6IrS_2PF_6$ (884.32); C, 38.03; H, 3.08; N, 9.50. Found: C, 38.04; H, 3.05; N, 9.48 %.

2.7. General procedure for the synthesis of dinuclear complexes ***5-8***

A mixture of starting metal precursor (0.1 mmol) and ligand pyrimidine based thienyl pyrazoles (**L1**) (0.1 mmol) and 2.5 equivalents of NH_4PF_6 were dissolved in dry methanol (15 ml) and stirred at room temperature for 8 hours (Scheme-3). The solvent was evaporated to dryness. The residue was then dissolved in dichloromethane and filtered through a bed of celite to remove excess NH_4Cl. The filtrate was concentrated to 1 ml and on the addition of excess hexane yellow solid precipitates out. The precipitate was further washed with diethyl ether and air-dried.

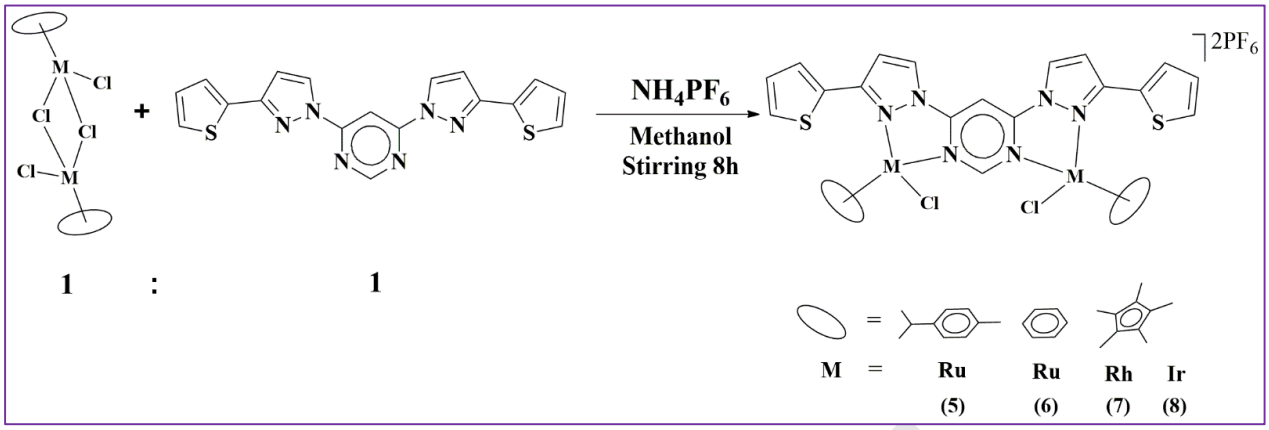

Scheme 3: Synthesis of complexes **5-8**

2.7.1. [{(p-cymene)RuCl}$_2$(μ-L1)](PF$_6$)$_2$ ***[5]***

Yield: 74%; IR (KBr, cm^{-1}): 2971 $\nu_{(C-H)}$, 1541 $\nu_{(C=N)}$, 1094 $\nu_{(C-N)}$, 960 $\nu_{(N-N)}$, 840 $\nu_{(P-F)}$, 776 $\nu_{(C-S)}$; ^{1}H NMR (400 MHz, $CDCl_3$, ppm) : 11.55 (s, 1H), 9.58 (s, 1H), 8.20 (s, 2H), 7.39 (d, 2H, *J* = 4Hz), 7.35 (d, 2H, *J* = 4Hz), 7.08 (t, 2H, *J* = 4Hz), 6.57 (s, 2H), 5.98 (d, 4H, *J* = 4Hz), 5.87 (d, 4H, *J* = 4Hz), 2.48 (sept, 2H), 1.92 (s, 6H), 1.15 (d, 12H, *J* = 4Hz); UV-Vis {Acetonitrile, λ_{max} nm (ε/10-4 M^{-1} cm^{-1})}: 224.97 (6.33), 269.96 (5.13), 350.94 (0.32). Anal. Calc for $C_{38}H_{40}Cl_2N_6Ru_2S_2P_2F_{12}$ (1207.87); C, 37.79; H, 3.34; N, 6.96. Found: C, 37.85; H, 3.40; N, 7.01 %.

2.7.2. [{(benzene)RuCl}$_2$(μ-L1)](PF$_6$)$_2$ ***[6]***

Yield: 71%; IR (KBr, cm^{-1}): 2998 $\nu_{(C-H)}$, 1588 $\nu_{(C=N)}$, 1118 $\nu_{(C-N)}$, 958 $\nu_{(N-N)}$, 843 $\nu_{(P-F)}$, 713 $\nu_{(C-S)}$; ^{1}H NMR (400 MHz, $CDCl_3$, ppm) : 9.24 (s, 1H), 8.51 (s, 1H), 7.55 (d, 2H, *J* = 4Hz), 7.41 (t, 2H, *J* = 4Hz), 7.15 (s, 2H), 6.59 (s, 2H), 6.10 (s, 12H), 5.87 (s, 2H); ^{13}C NMR (100 MHz, $CDCl_3$, ppm):160.56, 155.60, 144.95, 140.74, 128.85, 128.09, 127.26, 126.77, 105.56, 100.71, 85.71; UV-Vis {Acetonitrile, λ_{max} nm (ε/10-4 M^{-1} cm^{-1})}: 274.98 (5.99). Anal. Calc for

$C_{30}H_{24}Cl_2N_6Ru_2S_2P_2F_{12}$ (1095.66); C, 32.89; H, 2.21; N, 7.67. Found: C, 32.88; H, 2.24; N, 7.71 %.

*2.7.3. [{Cp*RhCl}$_2$(μ-L1)](PF$_6$)$_2$* ***[7]***

Yield: 68%; IR (KBr, cm^{-1}): 2992 $\nu_{(C-H)}$, 1605 $\nu_{(C=N)}$, 1080 $\nu_{(C-N)}$, 955 $\nu_{(N-N)}$, 845$\nu_{(P-F)}$, 719 $\nu_{(C-S)}$; ^{1}H NMR (400 MHz, $CDCl_3$, ppm) : 11.16 (s, 1H), 9.69 (s, 1H), 8.29 (s, 2H), 8.04 (d, 2H, *J* = 4Hz), 7.29 (d, 2H, *J* = 4Hz), 7.11 (t, 2H, *J* = 4Hz), 6.48 (s, 2H), 1.63 (s, 30H); ^{13}C NMR (100 MHz, $CDCl_3$, ppm): 161.96, 154.33, 143.47, 138.24, 134.90, 132.04, 127.48, 121.79, 108.98, 103.54, 98.11, 9.67; UV-Vis {Acetonitrile, λ_{max} nm (ε/10-4 M-1 cm-1)}: 229.98 (5.94), 269.96 (5.13), 395.02 (0.15). Anal. Calc for $C_{38}H_{42}Cl_2N_6Rh_2S_2P_2F_{12}$ (1213.56); C, 37.61; H, 3.49; N, 6.93. Found: C, 37.66; H, 3.52; N, 6.90 %.

*2.7.4. [{Cp*IrCl}$_2$(μ-L1)](PF$_6$)$_2$* ***[8]***

Yield: 60%; IR (KBr, cm^{-1}): 2997 $\nu_{(C-H)}$, 1613 $\nu_{(C=N)}$, 1077 $\nu_{(C-N)}$, 960 $\nu_{(N-N)}$, 843$\nu_{(P-F)}$, 722 $\nu_{(C-S)}$; ^{1}H NMR (400 MHz, $CDCl_3$, ppm) : 11.66 (s, 1H), 10.09 (s, 1H), 7.94 (s, 2H), 7.37 (d, 2H, *J* = 4Hz), 7.33 (d, 2H, *J* = 4Hz), 7.09 (t, 2H, *J* = 4Hz), 6.64 (s, 2H), 1.66 (s, 30H); ^{13}C NMR (100 MHz,$CDCl_3$, ppm): 162.69, 154.52, 149.93, 140.68, 134.80, 128.08, 127.37, 123.82, 106.63, 102.58, 99.33, 9.01; UV-Vis {Acetonitrile, λ_{max} nm (ε/10-4 M^{-1} cm^{-1})}: 285.41 (2.20), 350.16 (1.69). Anal. Calc for $C_{38}H_{42}Cl_2N_6Ir_2S_2P_2F_{12}$ (1392.18); C, 32.78; H, 3.04; N, 6.04. Found: C, 32.84; H, 3.00; N, 6.01 %.

3. RESULT AND DISCUSSION

3.1 Synthesis of complexes

Pyrimidine based ligands are widely used in medicinal chemistry for their anti-bacterial and antifungal properties. These pyrimidine based ligands have a variety of binding modes when

they coordinate with the metal atoms. In this work, we substituted thienyl pyrazole in the pyrimidine moiety (Scheme 1) and studied the way of bonding towards the d^6 metal complexes. The synthetic routes to pyrimidine-based pyrazoles are illustrated in scheme 1. These ligands can bind to the metal either through NN or NS but in these complexes sterically hindered N, N bonding occurred instead of a less sterically bonding mode of N, S site. Treatment of **L1** with the d^6 configured halo bridged metal dimers at room temperature in methanol results in the yellow-colored solution. After being stirred for one hour subsequent adding of NH_4PF_6 gave the complexes as yellow-colored precipitates. All these complexes are air and moisture stable, the solubility of these complexes is good in polar organic solvents like DCM, chloroform and acetonitrile whereas insoluble in solvents like hexane, and diethyl ether. All complexes are fully characterized by elemental analysis, ^{1}H NMR, ^{13}C NMR, IR, UV-Vis spectroscopy.

3.2 IR studies of metal complexes

Complexes **1-8** exhibits characteristic stretching frequencies for $\nu_{(C-H)}$, $\nu_{(C=N)}$, $\nu_{(C-N)}$, $\nu_{(N-N)}$, $\nu_{(C-S)}$ and $\nu_{(P-F)}$. The IR spectrum of the complexes was compared with that of the free ligand. The free ligand shows a characteristic stretching frequency at 1559 cm^{-1} for the $\nu_{(C=N)}$ whereas in the metal complexes the $\nu_{(C=N)}$ absorbs at higher frequency region in the range 1577-1613 cm^{-1}. Since all the complexes are cationic a characteristic stretching and bending frequencies for $\nu_{(P-F)}$ appeared as a sharp band around 844 cm^{-1} and 550 cm^{-1} respectively.

3.3 NMR studies of the complexes

The ^{1}H NMR spectra of ligand and complexes are depicted in figures S1-S8. The coordination of the ligand to the metal atom was further confirmed by carrying out the NMR analysis. In the metal complexes, the signals associated with the aromatic ligand protons were observed in the downfield region as compared to the free ligand which suggests the coordination

of the ligand to the metal atoms [35]. After the formation of complexes, the aromatic proton of the ligand was observed in the range 6.17-11.66 ppm which are downfield shifts. The aromatic proton signals of the *p*-cymene ligand in complexes **1** and **5** are observed as two doublets around 5.87- 6.06 ppm, one septet around 2.21-2.48 ppm for the methine protons of the isopropyl group and a singlet at 1.79 and 1.92 ppm for the methyl protons and doublet at 1.12-1.15 ppm for the isopropyl group. The benzene proton resonance in complexes **2** and **6** is observed as a singlet at 5.98 and 6.10 ppm respectively. In addition, a sharp singlet is observed for the rhodium and iridium complexes around 1.63-1.79 ppm for the methyl protons of the Cp* ligand. Upon the formation of mononuclear complexes, the two sides of the ligand are no longer equivalent as one side of the ligand bind to the metal center so the proton for both sides of the ligand was observed in different chemical shift whereas in dinuclear complexes the chemical environment for both sides are equivalent so it exhibited same shift. Furthermore, the formation of mononuclear and di-nuclear complexes is confirmed by the integral ratio of the ligand with respect to the precursor complexes

The ^{13}C NMR spectra of the complexes further justify the coordination of the ligands and formation of complexes. The ^{13}C NMR spectra of the representative complexes are provided in the supplementary information (figures S9-S14). The ^{13}C NMR spectra of the complexes displayed signals associated with the ligand carbons, *p*-cymene ligand carbons, methyl carbon of Cp* and ring carbon of Cp*. The aromatic carbons signals for the ligands were observed in the range of 166.26 to 102.58 ppm. The methyl, methine, and isopropyl carbon resonances of the *p*-cymene ligand were observed in the region around 17.94 - 30.87 ppm. Complex **2** and complex **6** displayed a sharp signal at 86.56 and 85.71 ppm for the carbon of the benzene ring. The signals associated with the ring carbons of the Cp* ligand in complex **4**, complex **7** and complex **8** were

observed at 97.27, 98.11 and 99.33 ppm respectively, in contrast, the methyl carbon resonances were observed as a sharp peak at 13.42, 9.67 and 9.01 ppm respectively. Overall results from the NMR spectral studies strongly support the formation of the metal complexes.

3.4 Ultraviolet-Visible spectra of the complexes

The electronic spectra of the complexes **1**-**8** along with the corresponding ligands **L1** have been recorded in acetonitrile solutions in the range 200-600 nm at a concentration of 10 μM and were depicted in figure S15. The free ligands and complexes exhibit two characteristic high intense absorption bands, peaks at around 277, 285 nm are due to n - π* transition, peaks in the range 230 nm are tentatively assigned to π→π* transitions. In addition, the complexes **1**-**8** exhibit a weak band or a small hump in the visible region at around 410 nm of the spectrum, which arises due to the excitation of electrons from metal t_{2g} level to the empty π* level of the ligand (MLCT). Such weak bands may be ascribed either from the low concentration of the solutions or obscured by the high intense bands.

3.5 Single-crystal X-ray structure determination of complexes

The molecular structures of some complexes were established by carrying out the single crystal analysis. The solid-state structures was established and the thermal ellipsoid plot along with crystallographic numbering schemes is depicted in Figure 1. The summary of the crystal data, data collection, and structure refinement parameters are summarized in Table 1, selected bond lengths, bond angles values are listed in Table 2.

By single-crystal X-ray diffraction studies, we were able to establish the coordination modes associated with these ligands. Complex **5** crystallized in the monoclinic crystal system with space group *C2/m*. X-ray crystallographic studies showed that complex **5** contained the cationic species of $[\{(p\text{-cymene})RuCl\}_2(\mu\text{-L1})]$ and counter anion contained two molecules of

PF_6^-. The crystal structure of complex **5** contains the disordered of acetone molecule in their solved structure. The coordination sites around the metal is occupied by the arene ligand (arene = *p*-cymene/benzene/Cp*) in a η^6/η^5 manner, terminal chloride and a chelating NN´- ligand, arene ligand occupies the three facial coordination sites acting as seat of "piano-stool" and nitrogen's donor atoms from pyrimidine and pyrazole ligand and terminal chloride acting as legs.

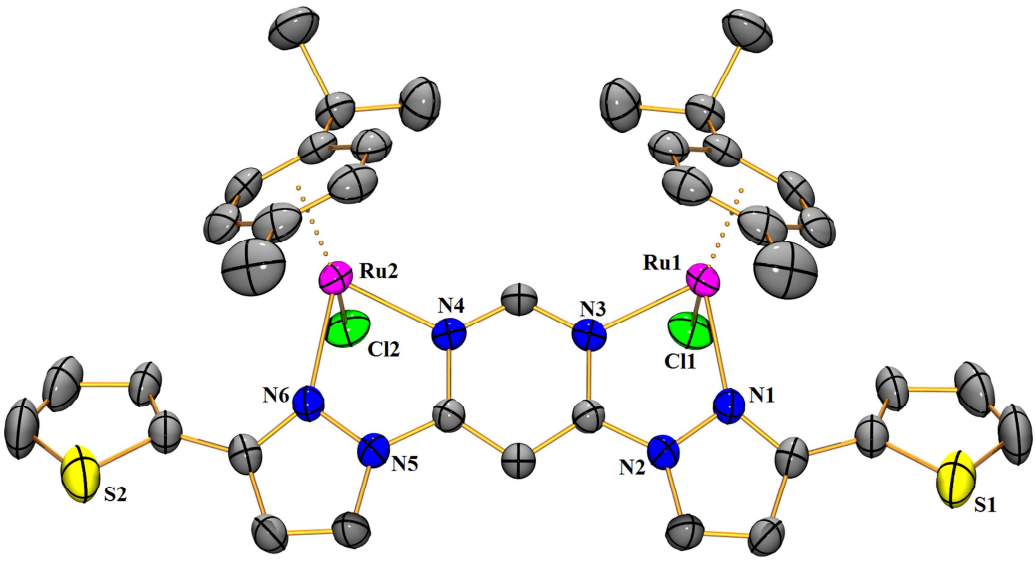

Figure 1. ORTEP plot of complex **5** with 50% probability thermal ellipsoids. Hydrogen atoms and counter ion (PF_6^-) are omitted for clarity

The molecular structure of this complex revealed that the ligands coordinated metal in a bidentate chelating NN´ fashion through pyrimidine nitrogen and pyrazole nitrogen. This coordination of the ligands in a bidentate manner led to the formation of a five-membered chelate ring with the metal center. The molecular structures of complex **5** revealed that the ligand is symmetry in which both sides of the ligand have essentially identical coordination geometry, and the corresponding bond lengths and bond angles are exactly the same. The arene ring is essentially planar and the metal to the centroid of the arene ring distances is { 1.682 (**5**) Å}. The

M-N1 bond length is shorter compared to M-N3 bond length which indicates that the metal binds strongly to the Nitrogen atom of the pyrazole rather than the nitrogen atom of the pyrimidine. The observed M-N and M-Cl bond lengths in these complexes are found to be in close agreement with reported complexes with nitrogen donor ligands [36]. The bond angle values N-M-Cl (M = Ru and Rh) are close to 90° which is consistent with the piano-stool arrangement of various donor groups about the metal atom [37].

3.6 Antibacterial activity

Antibacterial activities of the ligand and complexes have been tested against the Gram-positive *Staphylococcus aureus* and Gram-negative *Escherichia coli, Klebsiella pneumoniae* strains. The result was compared to the corresponding positive controls and the zone of inhibition (in mm) was given in Table 3. The histogram of the antibacterial activities of the complexes is shown in figure 2 and the Agar plates of complexes against the tested bacterial strains were shown in figure S16- S18. It has been observed that all the complexes displayed effective antibacterial activity against the tested organisms but ruthenium chelates have high antibacterial activity. The antibacterial activity of the starting metals precursor was found to be inactive as previously reported [38]. This specified that the antibacterial activity ascribed to the ligands and the metal complexes. The better activity for the metal chelates compared to the free ligands can be elucidated on the basis of chelation theory [39]. The activity of the metal complexes may also be engaged to the lipophilic character of the central metal atom which arose from the chelation pattern; this consequently favors the permeation *via* the lipid layer of the cell membrane [40]. The difference in the effectiveness of the complexes against the tested organisms is based on the ribosome of the microbial cells or the impermeability of the cells of microbes [41]. *In-vitro* assay results revealed that complex **2** (20 ± 0.76 mm), complex **6** (20 ±

0.96 mm) and complex **7** (20± 1.09 mm), has the highest potential against Gram-positive *Staphylococcus aureus*. Complex **6** showed the highest activity against Gram-negative *Escherichia coli* (17 ± 0.56 mm) and *Klebsiella pneumonia* (17 ± 0.86 mm). Even though all the studied complexes are active, but they did not reach the effectiveness of the positive control ciprofloxacin.

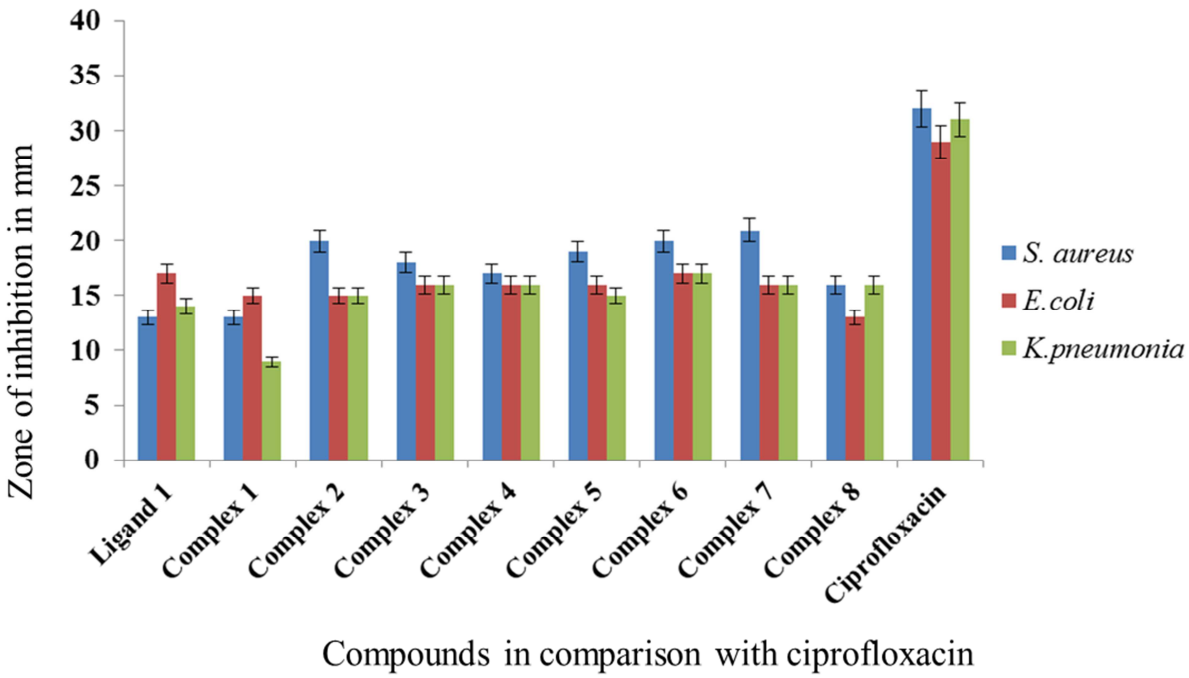

Figure 2: Histogram of the zone of inhibition (mm) of the ligand and complexes **1-8** in comparison with ciprofloxacin**.** All the complexes data are means (n = 3) ± Standard deviation of three replicates.

3.7 MIC and MBC

The minimum inhibitory concentration (MIC) and minimum bactericidal concentration (MBC) results were listed in Table 4 or Figure 3. The MIC and MBC values of ligand and complexes **1-8** ranged from 0.125 to 1.0 mg/ml against all the three bacterial organisms. The MIC and MBC values of complex **4**, complex **5** and complex **7** values ranged from 0.125 to 0.25

mg/ml for *S. aureus* and *Klebsiella Pneumoniae*. The values of complex **7** ranged from 0.25 to 0.5 mg/ml for *E. coli*. The MIC and MBC values of standard ciprofloxacin range from 0.031 to 0.062 mg/ml and 0.062 to 0.0125 mg/ml against the tested organisms. It was found that the MBC values attained for the ligand and complexes are twice higher than the corresponding MIC values. As the MBC values were twice to MIC values it can be concluded that the ligand and complexes are bacteriostatic rather than bactericidal.

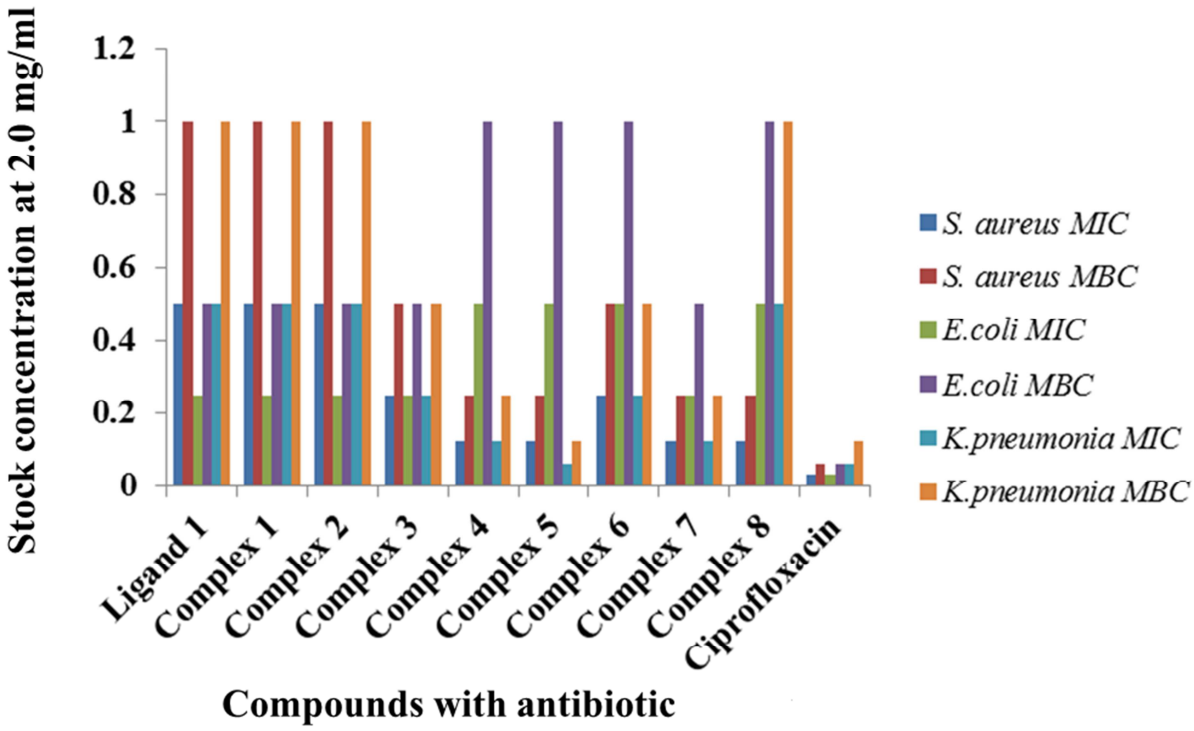

Figure 3: MIC and MBC of the ligand and complexes **1-8**.

Conclusion

In this study, we have successfully introduced a range of ruthenium, rhodium, and iridium half-sandwich d^6 metal complexes containing pyrimidine based thienyl pyrazoles ligand. The complexes are fully characterized by analytical and various spectroscopic methods and the

solid-state structure of complex **5** has been determined by single-crystal X-ray diffraction studies to confirm the binding mode of the ligand to the metal. All the complexes were isolated as cationic salts with PF_6^- as the counterion. The ligand understudy preferably binds to the metal in a bidentate NN´ manner using pyrimidine and a pyrazole nitrogen atom. All the eight complexes investigated in the present study were screened for their *in vitro* antibacterial activity against three human pathogens *viz.*, S. *aureus*, *E. coli*, and *K. Pneumoniae*. The antibacterial data showed that all the complexes have the capacity of inhibiting the metabolic growth of the investigated bacteria to different extents, which may indicate broad-spectrum properties;

Acknowledgments

Agreeda Lapasam acknowledges the financial support of CSIR-HRDG, New Delhi in the form of SRF-NET award no. 09/347(0223)/2017-EMR-I. We thank DST-PURSE SCXRD, NEHU-SAIF, Shillong, India for providing Single-crystal X-ray analysis and other spectral studies.

Appendix A. Supplementary data

Crystallographic data for the structural analysis has been deposited with the Cambridge Crystallographic Data Centre, CCDC **1967663** (Complex 5). Whole information can be attained free of charge by e-mailing data_request@ccdc.cam.ac.uk, or by contacting from The Cambridge Crystallographic Data Centre, 12 Union Road, Cambridge, CB21 EZ, UK(fax: +44 1223336033).

REFERENCE

[1] H.W. Boucher, G.H. Talbot, J.S. Bradley, Clin Infect Dis., 48 (2009) 1.

[2] H.W. Boucher, G.H. Talbot, J.S. Bradley, J.E. Edwards Jr, D. Gilbert, L.B. Rice, M. Scheld, B. Spellberg, J. Bartlett, IDSA Report on Development Pipeline, (2009) 48.

[3] K.J. Simmons, I. Chopra, C.W.G. Fishwick, Nat. Rev. Microbiol., 8 (2010) 501.

[4] S.H. van Rijt, P.J. Sadler, Drug Discovery Today, 14 (2009) 1089.

[5] P.S. Kuhn, V. Pichler, A. Roller, M. Hejl, M.A. Jakupec, W. Kandioller, B.K. Keppler, Dalton Trans., 44 (2015) 659.

[6] (a) J.M. Rademaker Lakhai, D. van den Bongard, D. Pluim, J.H. Beijnen, J.H.M. Schellens, Clin. Cancer Res. 10 (2004) 3717.

(b) C.G. Hartinger, S. Zorbas-Seifried, M.A. Jakupec, B. Kynast, H. Zorbas, B.K. Keppler, J. Inorg. Biochem. 100 (2006) 891.

[7] (a) C.G. Hartinger, P.J. Dyson, Chem. Soc. Rev. 38 (2009) 391.

(b) A. Bolhuis, L. Hand, J.E. Marshall, A.D. Richards, A. Rodger, J. Aldrich-Wright, Eur. J. Pharm. Sci., 42 (2011) 313.

(c) N.V. Kulkarni, A. Kamath, S. Budagumpi, V.K. Revankar, J. Mol. Struct., 106 (2011) 580.

(d) F. Li, Y. Mulyana, M. Feterl, J.M. Warner, J.G. Collins, F. R. Keene, Dalton Trans., 40 (2011) 5032.

[8] N. Turan, K. Buldurun, Y. Alan, A. Savci, N. Çolak, A. Mantarci, Res. Chem. Intermed., 45 (2019) 3525.

[9] (a) U. Schatzschneider, Advance in bioorganometallic chemistry, (2019) 173.

(b) F. Chen, J. Moat, D. McFeely, G. Clarkson, I.J. Hands-Portman, J.P. Furner-Pardoe, F. Harrison, C.G. Dowson, P.J. Sadler, J. Med. Chem. 61 (2018) 7330.

[10] A. Arafat, F. Adam, M.R. Razali, L.E.A. Hassan, M.B.K. Ahamed, A. Malik, S.A. Majid, J. Mol. Struct., 1130 (2017) 791.

[11] (c) P. Chellan, V.M. Avery, S. Duffy, J.A. Triccas, G. Nagalingam, C. Tam, L.W. Cheng, J. Liu, K.M. Land, G.J. Clarkson, I. Romero-Caneljn, P.J. Sadler, Chem. Eur. J., 24 (2018) 10078.

[12] D. Sun, Z. Mou, N. Li, W. Zhang, Y. Wang, E. Yang, W. Wang, J. Biol. Inorg. Chem., 21 (2016) 945.

[13] L. Cardo, I. Nawroth, P.J. Cail, J.A. Mc Keating, M.J. Hannon, Sci. rep. 8 (2018) 13342.

[14] A. Molter, S. Kathrein, B. Kircher, F. Mohr, Dalton Trans., 47 (2018) 5055.

[15] C.S. Freitas, A.C. Roveda Jr., D.R. Truzzi, A.C. Garcia, T.M. Cunha, F.Q. Cunha, D.W. Franco, J. Med. Chem., 58 (2015) 4439.

[16] (a) R.J. Bromfield, R.H. Dainty, R.D. Gillard, B.T. Heaton, Nature, 223(1969) 735.

[17] N. Farrel, B. James, R. Ugo, Transition Metal Complexes as Drugs and Chemotherapeutic Agents, Academic Press, Dordrecht, 1989.

[18] J. Mondal, A.K. Panigrahi, A.R. Khuda-Bukhsh, Austin Journal of Molecular and Cellular Biology, 1(2014) 1.

[19] (a) Z. Liu, P.J. Sadler, Acc. Chem. Res., 47 (2014) 1174.

(b) F. Chen, J. Moat, D. McFeely, J. Med. Chem., 61 (2018) 7330.

(c) L. Lu, L. Liu, W. Chao, Sci. Rep., 5 (2015) 1.

(d) S. Dave, N. Bansal, Int. J. Curr. Pharm. Res., 5 (2013) 1.

(e) Z. Almodares, S.J. Lucas, B.D. Crossley, Inorg. Chem., 53 (2014) 727.

(f) S.J. Lucas, R.M. Lord, R.L. Wilson, R.M. Phillips, V. Sridharan, P.C. McGowan, Dalton Trans., 41 (2012) 13800.

[20] T. Mukherjee, M. Mukherjee, B. Sen, S. Banerjee, G. Hundal, P. Chattopadhyay, J. Coord. Chem (2014) https://doi.org/10.1080/00958972.2014.945924.

[21] E.C. Constable, P.J. Steel, Coord. Chem. Rev., 93 (1989) 205.

[22] H. Ohki, K. Hirotani, H. Naito, S. Ohsuki, M. Minami, A. Ejima, Y. Koiso, Y. Hashimoto, Bioorg. Med. Chem. Lett., 12 (2002) 3191.

[23] H. Naito, S. Ohsuki, M. Sugimori, R. Atsumi, M. Minami, Y. Nakamura, M. Ishii, K. Hirotani, E. Kumazawa, A. Ejima, Chem. Pharm. Bull., 50 (2002) 453.

[24] B.P.R. Aradhyula, K. Gulati, N. Joshi, D.K. Deb, D. Rambabu, W. Kaminsky, K.M. Poluri, M.R. Kollipara, Inorg. Chim. Acta, 462 (2017) 223.

[25] (a) B.P.R. Aradhyula, I.L. Mawnai, W. Kaminsky, M.R. Kollipara, Inorg. Chim. Acta, 476 (2018) 101.

(b) B.P.R. Aradhyula, I.L. Mawnai, M.R. Kollipara, Z. Anorg. Allg. Chem., 645 (2019) 79.

(c) I.L. Mawnai, S. Adhikari, L. Dkhar, J.L. Tyagi, K.M. Poluri, M.R. Kollipara, J. Coord. Chem., 72 (2019) 294.

[26] D.D. Perrin, W.L.F. Armarego, Purification of Laboratory Chemicals, fourth ed., Butterworths Heinemann, London, 1996.

[27] M.A. Bennett, T.N. Huang, T.W. Matheson, A.K. Smith, G.B. Robertson, Inorg. Synth., 21 (1985) 74.

[28] M.A. Bennett, T.W. Matheson, G.B. Robertson, A.K. Smith, P.A. Tucker, Inorg. Chem., 19 (1980) 1014.

[29] A. Lapasam, O. Hussain, R.M. Phillips, W. Kaminsky, M. R. Kollipara, J. Organomet Chem. 880 (2019) 272-280.

[30] G.M. Sheldrick, Acta Crystallogr. Sect. A, 71(2015) 3.

[31] G.M. Sheldrick, Acta Crystallogr. Sect. C, 71(2015) 3.

[32] L.J. Farrugia, J. Appl. Crystallogr., 32 (1999) 837.

[33] (a) V. Banothu, A. Uma, Ch. Suvarnalaxmi, N. Chandrasekharnath, R. S. Prakasham and L. Jayalaxmi, Current Trends in Biotechnology and Pharmacy, 7 (2013) 782.

(b) V. Banothu, A. Uma, J. Lingam, Int. J. Pharm. Sci. 9 (2017) 192.

[34] V. Banothu, C. Neelagiri, A. Adepally, J. Lingam, K. Bommareddy, Pharm Biol., 55 (2017) 1155.

[35] (a) B.P.R. Aradhyula, A. Uma, T. Chiranjeevi, M.S. Bethu, B. Yashwanth, J.V. Rao, K.M. Poluri, M.R. Kollipara, Inorg. Chim. Acta, 453 (2016) 284.

(b) B.P.R. Aradhyula, N.R. Palepu, D.K. Deb, A. Uma, T. Chiranjeevi, B. Sarkar, W. Kaminsky, M.R. Kollipara, Inorg. Chim. Acta, 453 (2016) 126.

[36] (a) S. Adhikari, W. Kaminsky, M.R. Kollipara, J. Organomet. Chem. 848 (2017) 95.

(b) S. Adhikari, W. Kaminsky, M.R. Kollipara, J. Organomet. Chem. 836 (2017) 8.

[37] A. Lapasam, E. Pinder, R.M. Phillips, W. Kaminsky, M.R. Kollipara, J. Organomet. Chem., 899 (2019) 120887.

[38] A. Lapasam, L. Dkhar, N. Joshi, K.M. Poluri, M.R. Kollipara, Inorg. Chim. Acta, 484 (2019) 255.

[39] B.G tweedy, phytopathology, 55 (1964) 910.

[40] R. Prabhakaran, A. Geetha, M. Thilagavathi, R. Karvembu, V. Krishnan, H. Bertagnolli, K. Natarajan, J. Inorg. Biochem. 98 (2004) 2131.

[41] P.G. Lawrence, P.L. Harold, O.G. Francis, Antibiot. Chemother. 4 (1980) 1957

Table 1: Crystal data and structure refinement details of complexes

Complexes	**Complex 5**
Empirical formula	C_{88} H_{104} Cl_4 F_{24} N_{12} O_4 P_4 Ru_4 S_4
Formula weight	2648.03
Temperature (K)	294(2)
Wavelength (Å)	0.17073
Crystal system	Monoclinic
Space group	*C 2/m*
a (Å)/α (°)	16.1473(7)/90
b (Å)/β (°)	23.1541(8)/ 101.163(4)
c (Å)/γ (°)	14.4650(6)/90
volume (Å3)	5305.8(4)
Z	2
Density (calc) (Mg/m-3)	1.657
Absorption coefficient (μ) (mm-1)	0.894
F(000)	2664
Crystal size (mm3)	0.25 x 0.21 x 0.12
Theta range for data collection	3.954 to 28.923°
Index ranges	-20<=h<=21, -31<=k<=28, -19<=l<11
Reflections collected	11322
Independent reflections	6230 [R(int) = 0.0231]
Completeness to theta = 25.00°	98.9 %
Absorption correction	Semi-empirical from equivalents
Refinement method	Full-matrix least-squares on F^2
Data/restraints/parameters	6230/23/363
Goodness-of-fit on F^2	1.059
Final R indices [I>2sigma(I)]	R1 = 0.0402, wR2 = 0.0966
R indices (all data)	R1 = 0.0589, wR2 = 0.1097
Largest diff. peak and hole (e.Å^{-3})	0.623 and -0.462
CCDC No.	1967663

Structures were refined on F_0^2: $wR_2 = [\Sigma[w(F_0^2 - F_c^2)^2] / \Sigma w(F_0^2)^2]^{1/2}$, where $w^{-1} = [\Sigma(F_0^2)+(aP)^2+bP]$ and $P = [\max(F_0^2, 0)+2F_c^2]/3$.

Table 2: Selected bond lengths (Å) and bond angles (°) of complex **5**

Complex 5	
Ru-CNT	1.682
Ru-N1/N6	2.091(2)
Ru-N3 / N4	2.117(2)
Ru-Cl1/ Cl2	2.388(9)
N1-Ru1-N3 / N6-Ru2-N4	76.34(9)
N1-Ru1-Cl1 / N6-Ru2-Cl2	85.81(7)
N3-Ru1-Cl1 / N4-Ru2-Cl2	85.09(7)

CNT represents the centroid of the *p*-cymene ring)

Table 3: Antibacterial activity (Agar well) of ligand and complexes

S. No.	**Compound Names**	**Zone of inhibition (Diameter in mm) at concentration 200 µg**		
		S. aureus	***E. coli***	***K. pneumoniae***
1	**Ligand**	13 ± 0.16	17 ± 0.36	14 ± 0.16
2	Complex 1	13 ± 0.22	15 ± 0.28	09 ± 0.10
3	Complex 2	20 ± 0.76	15 ± 0.26	15 ± 0.21
4	Complex 3	18 ± 0.54	16 ± 0.34	16 ± 0.38
5	Complex 4	17 ± 0.48	16 ± 0.42	16 ± 0.29
6	Complex 5	19 ± 0.76	16 ± 0.39	15 ± 0.36
7	Complex 6	20 ± 0.96	17 ± 0.56	17 ± 0.86
8	Complex 7	21 ± 1.09	16 ± 0.85	16 ± 0.73
9	Complex 8	16 ± 0.35	13 ± 0.24	16 ± 0.54
10	Ciprofloxacin	32 ± 0.40	29 ± 0.15	31 ± 0.20

S. aureus = *Staphylococcus aureus*; E. coli = *Escherichia coli*; K. pneumoniae = *Klebsiella pneumoniae*, and Data are means (n = 3) ± Standard deviation of three replicates.

Table 4: MIC & MBC of ligand and complexes

S. No.	Compound Names	Stock concentration in 2.0 mg/ml					
		S. aureus		***E. coli***		***K. pneumoniae***	
		MIC	**MBC**	**MIC**	**MBC**	**MIC**	**MBC**
1	Ligand	0.5	1.0	0.25	0.5	0.5	1.0
2	Complex 1	0.5	1.0	0.25	0.5	0.5	1.0
3	Complex 2	0.5	1.0	0.25	0.5	0.5	1.0
4	Complex 3	0.25	0.5	0.25	0.5	0.25	0.5
5	Complex 4	0.125	0.25	0.5	1.0	0.125	0.25
6	Complex 5	0.125	0.25	0.5	1.0	0.125	0.25
7	Complex 6	0.25	0.5	0.5	1.0	0.25	0.5
8	Complex 7	0.125	0.25	0.25	0.5	0.125	0.25
9	Complex 8	0.125	0.25	0.5	1.0	0.5	1.0
10	Ciprofloxacin	0.031	0.062	0.031	0.062	0.062	0.125

S.aureus = *Staphylococcus aureus*; E. coli = *Escherichia coli*; K. pneumoniae = *Klebsiella pneumoniae*.

HIGHLIGHTS

1. Pyrimidine based thienyl pyrazole complexes of Ru, Rh and Ir have been isolated.
2. All the complexes shown potent activity against tested bacterial strain.
3. Both sides of the ligand having identical metal coordination geometry.

Professor K. Mohan Rao
Department of Chemistry
North Eastern Hill University
Shillong 793022

e mail: mohanrao59@gmail.com
mobile: 9436166937 (M)
tel. no. 0364 272 2620

The Editor

JOMC

Declaration of interest statement

'Declarations of interest: none'

Yours truly,

Mohan Rao Kollipara